J|A|C|S
ARTICLES
Published on Web 01/22/2004

Vibrational Signature of Charge Solvation vs Salt Bridge Isomers of Sodiated Amino Acids in the Gas Phase

Catherine Kapota,[†] Joël Lemaire,[‡,§] Philippe Maître,*[,‡] and Gilles Ohanessian*[,†]

Contribution from the Laboratoire des Mécanismes Réactionnels, UMR 7651 du CNRS, Ecole Polytechnique, 91128 Palaiseau CEDEX, France, Laboratoire de Chimie Physique, UMR 8000 du CNRS, Université de Paris-Sud, 91405 Orsay CEDEX, France, and Laboratoire pour l'Utilisation du Rayonnement Electromagnétique, UMR 130 du CNRS, Université de Paris-Sud, CLIO-BP34, 91405 Orsay CEDEX, France

Received June 27, 2003; E-mail: gilles.ohanessian@polytechnique.fr.

Abstract: The vibrational spectra of the gaseous sodium complexes of glycine (Gly−Na^+) and proline (Pro−Na^+) have been recorded in the spectral range 1150−2000 cm^{-1}. The complexes were formed by matrix-assisted laser desorption−ionization, introduced in the cell of a Fourier transform ion cyclotron resonance mass spectrometer, and their infrared spectra were recorded using photons of variable energy emitted by a free electron laser. Photon absorption was probed by the diminished intensity of the parent ion, due to its infrared-induced dissociation into bare sodium cation and the free amino acid and the appearance of Na^+. The observed absorption bands are assigned using *ab initio* computations of the IR spectra of the lowest energy isomers in each case. They provide the first experimental evidence that the salt bridge isomer is formed in the case of Pro−Na^+. In contrast, charge solvation by chelation of Na^+ between nitrogen and the carbonyl oxygen seems to be most favorable for Gly−Na^+, but a mixture of isomers cannot be ruled out in this case.

I. Introduction

α-Amino acids (AA) are known to be in their zwitterionic form in solution over a wide range of pH values.[1] In this isomer, acidic groups are deprotonated and the basic groups protonated. In the gas phase, however, all available evidence points to non-zwitterionic isomers being more favorable. Extensive studies on gaseous Gly have shown that the zwitterion is not even a local minimum on the potential energy surface.[2] There are however strong indications that the arginine zwitterion with a protonated side chain and deprotonated carboxyl group is of similar energy as its neutral counterpart without any charged sites.[3]

Two different ways may be envisioned to induce the neutral to zwitterion transition in the gas phase: either microsolvate the AA until a cluster of solvent molecules mimics the effects of a dilute solution[4] or else favor the zwitterion by attaching a charged species, such as an atomic metal cation, to the AA. In the latter case, the strong electrostatic interaction between the metal charge and the large dipole of the zwitterion may be enough to offset the intrinsic preference of the AA for the neutral isomer. The second approach is used in this work.

Several studies[5−15] have established that when a metal cation such as Na^+ is attached to an AA, several low-energy isomers can be formed, which fall into two broad categories: (i) charge solvation (CS), in which the metal charge is stabilized by

[†] Laboratoire des Mécanismes Réactionnels, Ecole Polytechnique.
[‡] Laboratoire de Chimie Physique, Université de Paris-Sud.
[§] Laboratoire pour l'Utilisation du Rayonnement Electromagnétique, Université de Paris-Sud.

(1) Voet, D.; Voet, J. G. *Biochemistry*, 2nd ed.; John Wiley and Sons: New York, 1995.
(2) (a) Ding, Y.; Krogh-Jespersen, K. *Chem. Phys. Lett*. **1992**, *199*, 261. (b) Yu, D.; Armstrong, D. A.; Rauk, A. *Can. J. Chem*. **1992**, *70*, 1762. (c) Nguyen, D. T.; Scheiner, A. C.; Andzelm, J. W.; Sirois, S.; Salahub, D. R.; Hagler, A. T. *J. Comput. Chem*. **1997**, *18*, 1609.
(3) (a) Price, W. D.; Jockusch, R. A.; Williams, E. R. *J. Am. Chem. Soc*. **1997**, *119*, 11988. (b) Chapo, C. J.; Paul, J. B.; Provencal, R. A.; Roth, K.; Saykally, R. J. *J. Am. Chem. Soc*. **1998**, *120*, 12956. (c) Rak, J.; Skursky, P.; Simons, J.; Gutowski, M. *J. Am. Chem. Soc*. **2001**, *123*, 11695.
(4) (a) Jensen, J. H.; Gordon, M. S. *J. Am. Chem. Soc*. **1995**, *117*, 8159. (b) Ding, Y.; Krogh-Jespersen, K. *J. Comput. Chem*. **1996**, *17*, 338. (c) Tunon, I.; Silla, E.;. Ruiz-Lopez, M. F. *Chem. Phys. Lett*. **2000**, *321*, 433. (d) Bandyopadhyay, P.; Gordon, M. S. *J. Chem. Phys*. **2000**, *113*, 1104. (e) Kassab, E.; Langlet, J.; Evleth, E.; Akacem, Y. *J. Mol. Struct. (THEOCHEM)* **2000**, *531*, 267. (f) Wang, W.; Pu, X.; Zheng, W.; Wong, N.-B.; Tian, A. *J. Mol. Struct. (THEOCHEM)* **2003**, *626*, 127.
(5) Jockusch, R. A.; Price, W. D.; Williams, E. R. *J. Phys. Chem. A* **1999**, *103*, 9266.
(6) (a) Bouchonnet, S.; Hoppilliard, Y. *Org. Mass Spectrom*. **1992**, *27*, 71. (b) Jensen, F. *J. Am. Chem. Soc*. **1992**, *114*, 9533. (c) Hoyau, S.; Ohanessian, G. *Chem. Eur. J*. **1998**, *4*, 1561. (d) Wyttenbach, T.; Witt, M.; Bowers, M. T. *Int. J. Mass Spectrom*. **1999**, *183*, 243.
(7) Hoyau, S.; Norrman, K.; McMahon, T. B.; Ohanessian, G. *J. Am. Chem. Soc*. **1999**, *121*, 8864.
(8) Marino, T.; Russo, N.; Toscano, M. *J. Phys. Chem. B* **2003**, *107*, 2588.
(9) Shoeib, T.; Hopkinson, A. C.; Siu, K. W. M. *J. Phys. Chem. B* **2001**, *105*, 12399.
(10) Hoyau, S.; Ohanessian, G. *Compt. Rend. Acad. Sci. Sér. IIc* **1998**, *1*, 795.
(11) Kapota, C.; Ohanessian, G. Unpublished results. See also: Hoyau, S.; Pélicier, J.-P.; Rogalewicz, F.; Hoppilliard, Y.; Ohanessian, G. *Eur. J. Mass Spectrom*. **2001**, *7*, 303.
(12) (a) Ryzhov, V.; Dunbar, R. C.; Cerda, B. A.; Wesdemiotis, C. *J. Am. Soc. Mass Spetrom*. **2000**, *11*, 1037. (b) Cerda, B. A.; Wesdemiotis, C. *Analyst* **2000**, *125*, 657. (c) Cerda, B. A.; Talley, J. M.; Wesdemiotis, C.; Ohanessian, G. *Chem. Eur. J*. **2002**, *8*, 1377. (d) Kish, M. M.; Ohanessian, G.; Wesdemiotis, C. *Int. J. Mass Spectrom*. **2003**, *227*, 509.
(13) (a) Jockusch, R. A.; Lemoff, A. S.; Williams, E. R. *J. Am. Chem. Soc*. **2001**, *123*, 12255. (b) Jockusch, R. A.; Lemoff, A. S.; Williams, E. R. *J. Phys. Chem. A* **2001**, *105*, 10929.
(14) Wyttenbach, T.; Witt, M.; Bowers, M. T. *J. Am. Chem. Soc*. **2000**, *122*, 3458.
(15) Moision, R. M.; Armentrout, P. B. *J. Phys. Chem. A* **2002**, *106*, 10350.

10.1021/ja036932v CCC: $27.50

Scheme 1

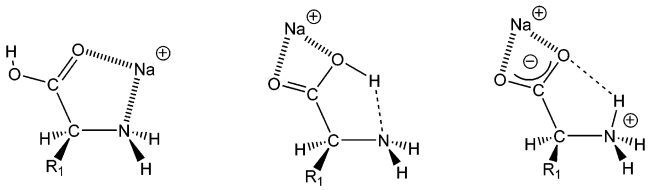

CS1 **CS2** **SB**

interaction with one, two, or more electron-rich site(s) of the AA in its neutral form, and (ii) salt bridges (SB), in which the metal charge interacts directly with the carboxylate group of the AA in its zwitterionic form (Scheme 1). The specificities of metal−AA interactions will determine whether CS or SB is most favorable in each case.

Several factors may influence the relative energies of CS and SB isomers:

(a) in a rough picture, the neutral → zwitterion transformation in the free AA may be viewed as a proton transfer from the carboxyl to a basic group (either the α-amino or a more basic side chain group if any, depending on the AA). The more basic the latter, the more favored the zwitterion will be. This reasoning was used to predict that Arg, the most basic of all 20 common AAs of living systems, might be more stable as a zwitterion.[3a] Further studies showed that this is not the case.[3b] However the lowest energy lying neutral and zwitterionic conformers were found to be close in energy.[3c] In such a case, attachment of a cation might well lead to a SB isomer that is more stable than the CS, and there exists indirect but compelling evidence that this is the case for Arg attached to heavy alkali metal ions.[5]

(b) The structural details of the best SB conformer may also be influential. For an optimum electrostatic stabilization, the protonated group should be able to approach the carboxylate in such a way as to make a quasi-linear array of charges with the metal ion. For long side chains with strongly basic groups, such as lysine and arginine, folding of the chain will allow the protonated end to approach the carboxylate but the arrangement of charges relative to the metal ion is not optimum. Computational studies on complexes of glycine with alkali cations reveal that protonation of the α-amino group is nearly ideal for such a purpose.[6] Therefore, the best candidate for a salt bridge might be the AA bearing the most basic α-amino group, that is, proline. It is indeed the case that Pro−Na^+ has been predicted, on the basis of *ab initio* calculations, to be most stable as a salt bridge, with a significant energy gap of ca. 6 kcal/mol with the most stable charge solvation isomer.[7] These results were recently confirmed by further, more detailed computations.[8]

(c) The electronic properties of the metal ion are also important. The above results for Pro−Na^+ have been extended to the closely related Pro−Li^+ and Pro−K^+ complexes, and again the SB was found to be most favorable.[8] Other computational studies have provided similar results for Pro−Ag^+;[9] however, Pro−Cu^+ [10] and Pro−Au^+ [11] are predicted to be different, with a CS isomer being the most stable.

There have been a number of experimental studies of cationized AAs using a variety of mass spectrometric techniques. Most have aimed at determining the metal ion−AA binding enthalpy and/or free energy. Successful results were obtained using the kinetic method,[12] dissociation kinetics induced by blackbody radiation,[13] ion mobility,[14] guided ion beam,[15] and metal ion exchange equilibrium[16] experiments. Assignment of the data to specific structures mostly relied on quantum chemical calculations, since none of the above methods can provide direct structural information. Several attempts were made to obtain indirect structural correlations, with some notable success.

(a) The kinetic method was used to compare the metal ion affinity of AAs and their methyl ester.[12b,c] Due to the methyl inductive effect, the ester has a larger metal ion affinity than the corresponding acid if both have similar structures. This is often the case if the acid leads to a CS isomer. However, when it is an SB, the analogous structure cannot be formed with the ester and the affinity order is reversed. This provides valuable clues as to the CS or SB structure of the metal−AA complex; however, it is rather indirect, and it may fail if the acid and the ester bear two different CS structures.

(b) Blackbody infrared radiation dissociation experiments were used to study the dissociation kinetics of metal−AA complexes into the bare metal ion and AA and to compare it to related cases which are known to have either CS or SB structures. Dissociation kinetics were shown to fall into two categories, which could be assigned to CS and SB types of isomers.[13] This indirect approach requires that structurally similar species with known structures exist, to which the species of interest must be compared.

However large the body of information already gathered, it is clear that a direct experimental characterization of the structure of cationized AA complexes is still lacking. It is the purpose of this paper to propose a new approach toward this goal, infrared spectroscopy of gaseous ions over a selected but wide spectral range. This technique has been made possible by the coupling of a radio frequency trap associated to a time-of-flight mass spectrometer and a free electron laser (FEL).[17] The FEL has two advantages over commercial tunable IR lasers: it has a much wider spectral range, and it provides a high peak power. Using this technique has provided a wealth of structural information on a broad variety of ion types, including ionized polycyclic aromatic hydrocarbons (PAHs) and metal clusters.[18] The technique has been made much more flexible and powerful recently by the coupling of a Fourier transform ion cyclotron resonance (FT-ICR) mass spectrometer to a FEL.[19] It provides the added value of trapping the ions for long times, which makes cooling possible and allows the gas-phase synthesis of new ions via gas-phase ion−molecule chemistry. This experimental setup has already been used to record the infrared spectra of organometallic complexes such as alkene−Fe^+ [19a] and to characterize the structure of reactive intermediates involved in the activation of methane by Ta^+ [20] and also of organic ions

(16) (a) Gapeev, A.; Dunbar, R. C. *J. Am. Chem. Soc.* **2001**, *123*, 8360. (b) Dunbar, R. C. posters presented at the 6th and 7th Gordon Conference on Structures, Energetics and Reaction Dynamics of Gaseous Ions, Ventura, CA, March 2001 and March 2003.
(17) Oomens, J.; van Roij, A. J. A.; Meijer, G.; von Helden, G. *Astrophys. J.* **2000**, *542*, 404.
(18) (a) Oomens, J.; Meijer, G.; von Helden, G. *J. Phys. Chem. A* **2001**, *105*, 8302. (b) Oomens, J.; Sartakov, B. G.; Tielens, A.; Meijer, G.; von Helden, G. *Astrophys. J.* **2001**, *560*, L99. (c) van Heijnsbergen, D.; von Helden, G.; Meijer, G.; Maître, P.; Duncan, M. *J. Am. Chem. Soc.* **2002**, *124*, 1562.
(19) (a) Lemaire, J.; Boissel, P.; Heninger, M.; Mauclaire, G.; Bellec, G.; Mestdagh, H.; Simon, A.; LeCaër, S.; Ortega, J. M.; Glotin, F.; Maitre, P. *Phys. Rev. Lett.* **2002**, *89*, 273002−1. (b) Maitre, P.; LeCaër, S.; Simon, A.; Jones, W.; Lemaire, J.; Mestdagh, H.; Heninger, M.; Mauclaire, G.; Boissel, P.; Prazeres, R.; Glotin, F.; Ortega, J. M.; *Nucl. Instrum. Methods A* **2003**, *507*, 541.
(20) MacAleese, L.; Simon, A.; Lemaire, J.; Boissel, P.; Maitre, P. Manuscript in preparation.

suchas protonated benzene.[21] This experimental setup is used here to probe the structures of gaseous sodium complexes of AAs. As representative cases, we studied Gly−Na^+ and Pro−Na^+, which are expected to form CS and SB isomers, respectively.

Gas-phase ions are produced in much too small quantities to measure the absorption of IR photons directly. Therefore, the absorption must be probed by a process induced by the absorption. Taking advantage of the capabilities of the mass spectrometer, a readily observable process is ion fragmentation, leading to a decreased intensity of the parent ion signal and the appearance of a fragment ion signal. In the present case, we monitored the fragmentation reaction shown in eq 1 as a function of photon energy:

$$AA{-}Na^+ \rightarrow Na^+ + AA \quad (1)$$

On the basis of computed AA−Na^+ binding energies, a single IR photon carries too small an energy to induce this fragmentation for any AA: the weakest binder is Gly, for which computations indicate that the binding enthalpy is ca. 37 kcal/mol. Therefore, we probe an InfraRed MultiPhoton Dissociation (IRMPD) process. It has been shown that IR−FEL are particularly well suited for this particular IR spectroscopy, since its fluence is so high that an ion can absorb several photons until it acquires enough internal energy to dissociate, via reaction 1 in the present case.

II. Experimental and Computational Section

1. Sample Preparation. Gaseous AA−Na^+ ions were produced just outside the ICR cell by matrix-assisted laser desorption ionization (MALDI) with a pulsed Nd:YAG laser at tripled frequency, delivering 355 nm photons. The best AA−Na^+ signal was obtained with a layered sample prepared following the sandwich technique.[22] The first layer contained 15 μL of the matrix, dissolved at a 3.75×10^{-2} mol L^{-1} concentration (see below). The second layer contained 5 μL of an aqueous solution of NaCl at a concentration of 2.5×10^{-2} mol.L^{-1}. The AA of interest was deposited as a third layer in the same conditions as NaCl, and a final layer of matrix identical to the bottom layer was added on top. Each new layer was let dry before the next was added; however, it is likely that some dissolution occurred. The matrix:NaCl:AA:matrix relative molar fractions in the sample were 4.5:1:2:4.5. Both 2,5-dihydroxy benzoic acid (DHB) in water and 4-hydroxy-α-cyano cinammic acid (HCCA) in a 1:3 v/v water−acetone solution were used as matrices. This choice was based on the relative sodium affinities of matrix molecules[23] and the AA of interest.[12d] The best spectra were obtained with HCCA for Pro−Na^+ and with DHB for Gly−Na^+.

2. Infrared Free Electron Laser Parameters. The FEL CLIO[26] is based on a 10−50 MeV electron linear accelerator followed by an ondulator placed in an optical cavity. The broadly tunable output (3−120 μm) and the high peak power makes it well suited for IR multiphoton dissociation studies. In our case the long-wavelength cutoff was ca. 19 μm due to the absorption of the ZnSe entrance window. The FEL output consists of 8 μs long macropulses fired at a repetition rate of 25 Hz. Each macropulse contains 500 micropulses, each a few picoseconds long. The mean IR power was about 500 mW, corresponding to micropulse and macropulse energies of 40 μJ and 20 mJ, respectively, and to a peak power of ca. 20 MW.

For a given electron energy, continuous tunability over a large spectral range ($\Delta\lambda/\lambda = 2.5$) is obtained by scanning the ondulator gap. The FEL bandwidth can be adjusted by tuning the length of the optical cavity. The laser wavelength profile was monitored while recording the spectra with a monochromator associated with a spiricon. In our case, the relative laser bandwidth was less than 0.5% of the central wavelength.

3. Operating Conditions. The experimental setup has been described in detail previously.[19b] It features an easily transportable FT-ICR-MS, MICRA,[28] which owes its compactness to the use of a 1.24 T permanent magnet made of an assemblage of Halbach cylinders.[29] The ICR cell is cubic like ($2 \times 2 \times 2$ cm), where each excitation electrode has been replaced by a set of four interconnected electrodes to provide optical access to the IR FEL.

The MALDI sample was deposited on a metallic holder (Cu/Ni alloy), which was mounted just outside the ICR cell, 6 mm away from the middle of the nearest trapping plate. The ions formed by the MALDI process enter the ICR cell, collinearly with the magnetic field, through a 5 mm diameter hole. A 3.5 V potential was applied to the trapping plates, and the target holder was maintained to a static potential, tuned to 1.8 V, so as to optimize the AA−Na^+ ion signal. Furthermore, the voltage of the entrance trapping plate was pulsed down to 0 V for 25 μs just after the laser pulse in order to favor ion entrance into the cell and then back to 3.5 V for trapping.

The infrared laser beam, perpendicular to the magnetic field, is focused in the middle of the ICR cell with a 1 m focal length spherical mirror. The laser beam waist at the focal point is probably smaller than the ion cloud dimensions. Nevertheless, provided that an irradiation time of 1s or more is used, photofragmentation ratios as high as 80% indicate that all ions eventually interact with the IR beam. The irradiation time is set by a fast electromechanical shutter, synchronized with the FEL, that allows for the selection of a given number of macropulses.

In the present study, AA−Na^+ ions of interest were mass selected 600−800 ms after their formation, then irradiated with the IR beam for 3 s (Pro−Na^+) or 1 s (Gly−Na^+), and the resulting ion signal was detected after the end of IR irradiation. Such a sequence followed by a quench was repeated 25 times, and the mass spectrum was the Fourier transform of the accumulated ion signal. In the case of Pro−Na^+, the IR laser wavenumber was increased by 10 cm^{-1} between two consecutive points. Due to difficulties to produce Gly−Na^+ ion, the corresponding IRMPD spectrum is the result of a multiple scans, with a smaller wavenumber spacing (10 cm^{-1}) near the IRMPD bands.

The IRMPD spectra presented in this paper are not corrected for variation of the laser fluence (F). The dependence of the IRMPD dissociation rate with the laser fluence is not a simple function. Approximation by a power law F^n has been used with values of n ranging between 1[19a] and 2.[18b] However, n may depend on the range of fluence, the nature of the ion, and probably also upon the IR-active mode which is resonantly excited. Therefore, no corrections were applied here, but one should keep in mind that the IRMPD process is probably favored by a higher fluence on the long wavelength side, considering that the monitored average FEL power was remarkably stable during these experiments.

4. Computational Details. The potential energy surfaces of Gly−Na^+ and Pro−Na^+ were computed at the MP2/6-31G* and

(21) Jones, W.; Boissel, P.; Chiavarino, B.; Crestoni, M. E.; Fornarini, S.; Lemaire, J.; Maître, P. *Angew. Chem., Int. Ed. Engl.* **2003**, *42*, 2057.
(22) Kussmann, M.; Nordhoff, E.; Rahbek-Nielsen, H.; Haebel, S.; Rossel-Larsen, M.; Jakobsen, L.; Gobom, J.; Mirgorodskaya, E.; Kroll-Kristensen, A.; Palm, L.; Roepstorff, P. *J. Mass Spectrom.* **1997**, *32*, 593.
(23) (a) Ohanessian, G. *Int. J. Mass Spectrom.* **2002**, *219*, 577. (b) Zhang, J.; Knochenmuss, R.; Stevenson, E.; Zenobi, R. *Int. J. Mass Spectrom.* **2002**, *213*, 237. (c) Zhang, J.; Ha, T.-K.; Knochenmuss, R.; Zenobi, R. *J. Phys. Chem. A* **2002**, *106*, 6610.
(24) Gaussian98, revision A.6; Frisch, M. J., *et al*.; Gaussian, Inc.: Pittsburgh, PA, 1998.
(25) Black, J.; Yablonovitch, E.; Bloembergen, N.; Mukamel, S. *Phys. Rev. Lett.* **1977**, *38*, 1131.
(26) Prazeres, R.; Glotin, F.; Insa, C.; Jaroszynski, D.; Ortega, J. M. *Eur. Phys. J. D* **1998**, *3*, 87.
(27) Kerstel, E. R. Th.; Lehmann, K. K.; Mentel, T. F.; Pate, B. H.; Scoles, G. *J. Phys. Chem.* **1991**, *95*, 8282.
(28) Mauclaire, G.; Lemaire, J.; Boissel, P.; Bellec, G.; Héninger, M. *Eur. J. Mass Spectrom.* **2003**, in press.
(29) Coey, J. M. D. *J. Magn. Magn.c Mater.* **2002**, *248*, 441.

B3LYP/6-31G* levels. Optimized geometries and relative energies obtained at identical or similar levels for the low-lying energy minima have been reported previously for Gly−Na^+ [6] and Pro−Na^+ [7,8] and are not repeated here. The vibrational spectra obtained at the same levels were used to interpret the recorded spectra. All calculations used the Gaussian98 package.[24] The calculated band intensities were convoluted assuming a Lorentzian profile with a 50 cm^{-1} full-width at half-maximum.

Hybrid DFT methods such as B3LYP have been shown to outperform local or gradient-corrected DFT, as well as MP2, in predicting the infrared intensities,[30] and an average absolute difference of 20−25 km mol^{-1} with the highest level *ab initio* method can be expected using B3LYP. Calculated frequencies are in general blue-shifted compared to the experimental ones. Provided the use of an appropriate scaling, hybrid DFT methods have been shown to be very efficient in producing the observed fundamental frequencies, and an average absolute difference of 33 cm^{-1} can be expected using B3LYP.[31] Sophisticated schemes for scaling the force constants rather than the frequencies have been developed, but their use is delicate since they strongly rely on the choice of internal coordinates. To account for the larger anharmonicity of the high-frequency modes, Schlegel and co-workers proposed a "dual-scaling": one scaling factor low- energy modes (<1800 cm^{-1}) and the other for the high-energy ones, essentially involving H stretches. This dual-scaling approach suggests that the low-energy modes are intrinsically better described than the high-energy ones: at the B3LYP level and provided the use of a large basis set, the scaling of the frequencies lower (higher) than 1800 cm^{-1} is 0.9927 (0.9659) while the uniform scaling factor is 0.9726. Similar conclusions were drawn at other levels of theory including MP2. Considering, in addition, that uniform scaling factors of 0.943 (0.9614) have been proposed for MP2 (B3LYP) using the 6-31G* basis set,[32] scaling factors of 0.96 and 0.98 were applied in the present work (1000−2000 cm^{-1}) to MP2/6-31G* and B3LYP/6-31G* frequencies, respectively. After applying these scalings, both sets of frequencies and intensities were very similar. It should be noted that the same scaling factor (0.98) was derived from the comparison of experimental and B3LYP/6-31G* frequencies in the 800−1800 cm^{-1} range of the IRMPD spectra of Fe(I) complexes.[19]

5. Other Accessible Spectral Ranges. The 1000−2000 cm^{-1} range has been chosen because it is in this region that calculations predict the most intense and well-separated bands. Indeed, in the 100−1000 cm^{-1} region there are numerous and less intense bands, making it difficult to interpret the spectrum. The 2000−3300 cm^{-1} region corresponds to the OH and NH stretching modes, so it seems structurally specific and therefore worth probing. However, there is always coincidence of several bands, for example, in the case of Gly−Na^+ the N−H stretching band of the SB isomer is in resonance with the O−H stretching band of CS2. Thus, the study of these regions would probably not bring any supplementary information.

6. IR Spectra of Deuterated Species. The spectra of some deuterated isotopomers of Gly−Na^+ and Pro−Na^+ have been simulated. We have only considered amino acids deuterated at nonexchangeable positions (CH_2), since it would be impossible to produce gaseous ions deuterated at exchangeable positions without the use of deuterated solvents and matrices. Thus, only d_2-Gly−Na^+ and d_7-Pro−Na^+ spectra were computed. The intensities of CD_2 (or CH_2) bending and stretching modes are weak, because of the small electronegativity difference between carbon and hydrogen. In conclusion, it appears that the study of deuterated species cannot be a complement to the assignment of spectra in these cases.

III. Results

1. Experimental Results. The absorption of multiple IR photons by the AA−Na^+ complexes is probed by their disappearance as a function of photon energy, due to the fragmentation reaction to form AA and Na^+ (eq 1). Monitoring the intensity of Na^+ relative to the total ion signal due to Na^+ and Pro−Na^+ leads to the IR spectrum shown in Figure 1a. Two main features are apparent: a broad signal between 1300 and 1430 cm^{-1} and another intense signal, with two partly resolved bands, between 1600 and 1750 cm^{-1}. Monitoring eq 1 for the Gly−Na^+ complex yielded an IR spectrum of lower quality than for Pro−Na^+ (Figure 2a). It may be seen that an intense feature exists between 1670 and 1800 cm^{-1}. A series of points showing one or several absorptions between 1150 and 1400 cm^{-1} is also apparent in the experimental spectrum. There is also a small feature in the 1400−1500 cm^{-1} range.

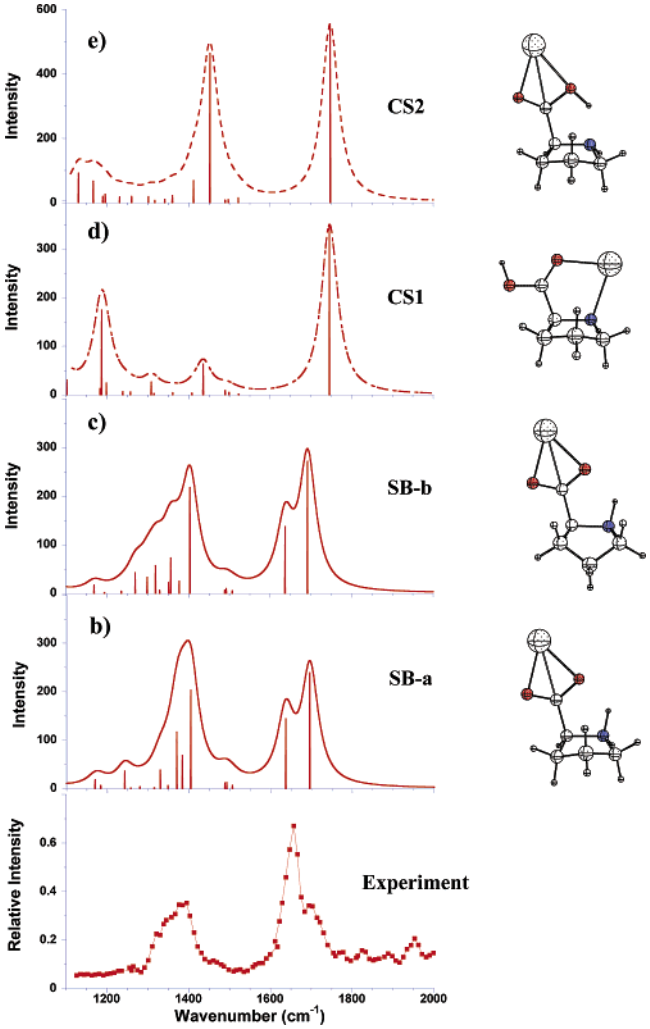

Figure 1. IRMPD spectrum of Pro−Na^+ (a). IR spectra and structures of the lowest energy Pro−Na^+ isomers, computed at the B3LYP/6-31G* level (b−e).

2. Low-Energy Isomers of Gly−Na^+ and Pro−Na^+. The low-energy isomers of both Gly−Na^+ and Pro−Na^+ have been studied previously, together with the transition states for some of their interconversions.[6−8] In both cases, the most favorable modes of attachment of the sodium ion to the AA are the same, although their energetic order is different. For Gly−Na^+, all computational levels indicate that the most stable isomer is CS1, in which the ion chelates Gly between nitrogen and the carbonyl oxygen. The SB and CS2 isomers lie 2−2.5 kcal/mol higher in energy, and other isomers are less stable. Pro−Na^+ differs from

(30) Halls, M. D.; Schlegel, H. B. *J. Chem. Phys.* **1998**, *109*, 10587.
(31) Halls, M. D.; Velkovski, J.; Schlegel, H. B. *Theor. Chem. Acc.* **2001**, *105*, 413.
(32) Scott, A. P.; Radom, L. *J. Phys. Chem.* **1996**, *100*, 16502.

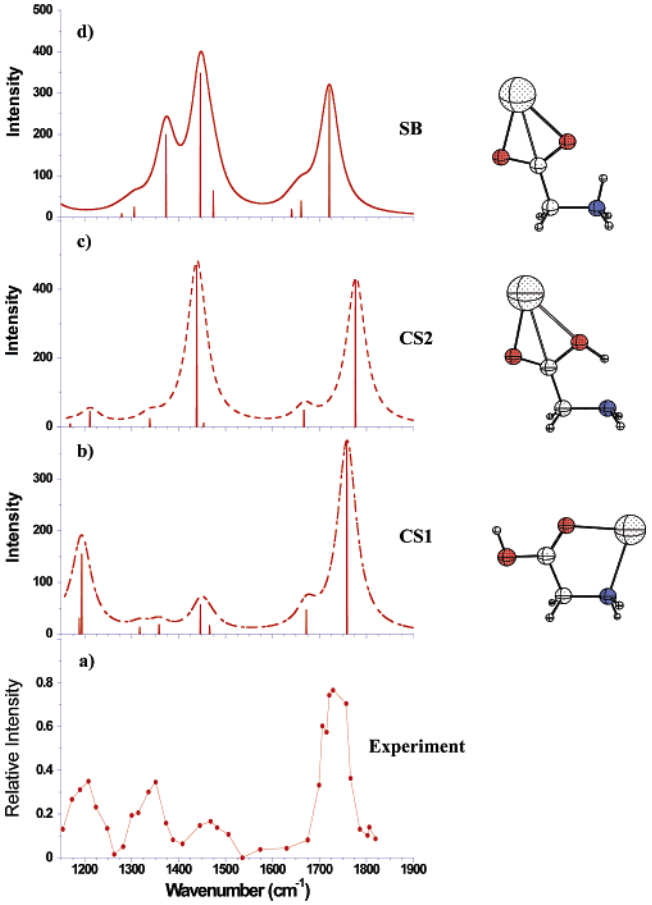

Figure 2. IRMPD spectrum of Gly−Na^+ (a). IR spectra and structures of the lowest energy Pro−Na^+ isomers, computed at the B3LYP/6-31G* level (b−d).

Gly−Na^+ in several significant ways. First, the SB isomer is the most stable, followed by CS1, which lies ca. 5 kcal/mol higher in energy. Second, as shown by Russo *et al.*,[8] each isomer exists as a pair of conformers differing by the puckering orientation of the five-membered ring. For each isomer, the energy difference between the two conformers is less than 1 kcal/mol, and they are connected by transition states with energy barriers of less than 3 kcal/mol. Third, the CS2 isomer exists as a very shallow minimum. It was impossible to locate CS2 on the MP2/6-31G* potential surface. Russo *et al.*[8] found it at the B3LYP/6-311++G** level; however, attempts to localize the transition state for proton transfer leading to SB were unsuccessful. We were able to locate both CS2 and this TS at the B3LYP/6-31G* level, and the TS was found to lie 0.3 kcal/mol higher than CS2 at the B3LYP/6-311+G(2d,2p)//B3LYP/6-31G* level. However, when thermal corrections at 298 K are included, it is found to lie 1.2 kcal/mol *below* CS2. This clearly indicates that CS2 lies on a rather flat portion of the potential surface and corresponds to a very shallow minimum at best. As for Gly−Na^+, other minima exist at higher energies, typically more than 10 kcal/mol higher than SB.

3. Assignment of the Computed IR Absorption Spectra of Pro−Na^+ Isomers. The simulated IR spectra and structures of the low-lying isomers of Pro−Na^+ are presented in Figure 1. Those for the two conformers of SB are shown in Figure 1b and 1c; those for CS1 and CS2 are shown in Figure 1d and 1e, respectively. The spectra of the second conformers of CS1 and CS2, corresponding to puckering inversion of the five-membered ring, are omitted for clarity. As mentioned in the Experimental and Computational Section, these IR absorption spectra are derived from a convolution of the calculated band intensities. The positions and intensities of the main bands are given in Table 1. The spectra of both CS isomers have two common bands. The strongest around 1740 cm^{-1} corresponds to the C═O stretch, while the second corresponds to the COH bend near 1450 cm^{-1}. The latter is much more intense for CS2 than for CS1. The CS1 spectrum presents another strong band at 1197 cm^{-1} due to the C−OH stretch. In the case of CS2, that absorption is much less intense. In comparison with the CS spectra, those for the conformers of SB are very different. In the 1600−1750 cm^{-1} range, two bands are predicted for SB instead of one for CS1 and CS2. A normal-mode analysis reveals that the two bands of SB display components on both the NH_2 scissoring (δNH_2) and the antisymmetric combination of C═O stretches ($\nu^{as}CO_2$), the less intense at 1637 cm^{-1} presenting a larger component on δNH_2, the most intense at 1696 cm^{-1} corresponding to $\nu^{as}CO_2$ mode. A group of peaks exists between 1300 and 1450 cm^{-1}, the most intense of which is associated with the symmetric combination of C═O stretches with the others being combinations of ring CH_2, CH, and NH_2 bendings.

Table 1: Measured (left column) and Calculated Vibrational Spectra for Pro−Na^+ [a]

Wavenumber (cm^{-1})		Calculated Intensity (km/mol)				Vibrational Mode
Experimental	Calculated	CS1	CS2	SB-a	SB-b	
	1131		92			νC-OH
	1167		67			τC-OH
	1187	174				νC-OH
1306	1319				57	Ring deformation[a]
	1357				73	
	1370			117		
	1384			68		
1429	1403				218	ν^sCO_2
	1404			203		
	1412		68			τNH
	1436	63				δCOH
	1452		465			
1656	1637				137	δNH_2
	1637			144		
1698	1692				271	$\nu^{as}CO_2$
	1696			239		
	1745	349				νC=O
	1747		550			

[a] Mode mainly localized on the five-membered ring, i.e., combination of τNH_2, τCH_2, ωCH_2, and τCH.

4. Assignment of the Computed IR Absorption Spectra of Gly−Na^+ Isomers. The simulated IR spectra and structures of the low-lying CS1, CS2, and SB isomers of Gly−Na^+ are displayed in Figure 2b, c, and d, respectively**,** and the positions of the most intense calculated IR bands are given in Table 2, along with their corresponding intensities.

As for Pro−Na^+, CS1 and CS2 share some common bands: the C−OH stretch near 1200 cm^{-1}, COH bend near 1440 cm^{-1}, NH_2 scissoring near 1670 cm^{-1}, and C═O stretch near 1760 cm^{-1}. The CS1 and CS2 spectra remain easily distinguishable because of the very different relative band intensities, especially

Table 2: Measured (left column) and Calculated Vibrational Spectra for Gly−Na^+

wavenumber (cm^{-1})		calculated intensity (Km/mol)			
experimental	calculated	CS1	CS2	SB	vibrational mode
	1189	30			$\tau NH_2 + \tau CH_2$
1204	1195	154			$\nu C-OH$
	1211		44		
	1306			24	$\omega NH_2 + \omega CH_2$
	1318	13			$\omega NH_2 + \omega CH_2$
	1339		23		ωCH_2
1351	1359	18			$\tau NH_2 + \tau CH_2$
	1373			199	$\nu^s CO_2$
	1439		469		$\delta C-OH$
1466	1446	56			
	1446			348	NH_3 umbrella
	1474			63	δCH_2
	1662			39	NH_3 bending
	1667		48		δNH_2
	1672	46			
	1721			309	$\nu^{as} CO_2$
1727	1759	370			$\nu C=O$
	1778		426		

in the 1300−1400 cm^{-1} region. The spectrum of isomer SB presents three characteristic bands, one at 1720 cm^{-1} corresponding to the antisymmetric combination of C−O stretches and two overlapping bands at 1446 and 1373 cm^{-1} corresponding to the NH_3 umbrella mode and the symmetric combination of C−O stretches, respectively. Contrary to the case of Pro−Na^+, distinguishing between SB and CS cannot be based on the 1650−1800 cm^{-1} zone since there are now two bands for all isomers, corresponding to NH_2 scissoring and combination of CO stretches.

IV. Discussion

A satisfactory agreement between the IRMPD and IR linear absorption spectra has been observed for a large variety of ions.[17−19,21] Thus, despite the multiple photon character of the IRMPD process, it is generally believed that the relative intensities of the bands in the IRMPD spectrum are governed by the absorption of the few first photons. This early stage of the IRMPD which occurs within the discrete regime[25] is critical, and no fragmentation occurs unless the first photon is resonant with a vibrational transition of the ion. Subsequent excitation occurs within the quasi-continuum regime in which the density of states is so high that the vibrational energy is rapidly randomized among all the modes of the molecule. Nevertheless, deviations from the linear absorption spectrum may be observed depending on the transition between these two regimes. Such deviation is expected for small ions for which the density of vibrational states is too low to allow for a fast energy redistribution. Vibrational couplings are also important, and it has been shown, for instance, that heavy atoms[27] may severely increase the lifetime of excited vibrational states, thereby decreasing the IRMPD efficiency. Furthermore, as cross-anharmonicities increase as a function of the internal energy, each vibrational transition is expected to be more and more red-shifted and broadened. As a result, the position of the peak maximum on the IRMPD spectrum is generally slightly red-shifted with respect to the corresponding maximum of the linear absorption spectrum.

1. Assignment of the Experimental IR Absorption Spectrum of Pro−Na^+. The assignment of the IRMPD spectrum of Pro−Na^+ is based on its comparison to the spectra computed for the various isomers described above. To make the comparison easier, the absorption cross-section is represented in Figure 1, assuming a Lorentzian profile for each calculated infrared band. As long as one considers only the relative positions of the two IRMPD broad bands, they are in better agreement with the two SB conformers (Figure 1b and c) than with the two CS isomers. Thus, a tentative assignment of the observed bands is proposed in Table 1 based on the calculated IR spectra of the SB isomers. As recalled above, the multiple photon character of the IRMPD process is expected to lead to some deviations from the relative intensities of the linear absorption spectrum (see discussion below), and this might be the case in the 1600−1750 cm^{-1} region.

If one considers the IRMPD experimental feature between 1100 and 1500 cm^{-1}, it does not show the principal signature of the CS1 isomer. Indeed, the intense C−OH stretch band at 1197 cm^{-1} of isomer CS1 (Figure 1d) is not observed experimentally. Isomer CS2 presents a strong absorption at 1450 cm^{-1}; however, there is only one mode with significant intensity in this region, which would lead to a much narrower feature than that experimentally observed. Furthermore, it has been found that CS2 is at best a very shallow minimum on the potential surface; therefore, it is unlikely to be observable in significant intensity. On the other hand, the computed spectra for the two conformers of SB are in fair agreement with the broad experimental feature. The broad character of the experimental signal between 1300 and 1450 cm^{-1} could be the result of the excitation of Pro−Na^+ through the various ring deformations of SB structures, and the maximum of the IRMPD rate could be attributed to the contribution of the $\nu^s CO_2$ at 1404 cm^{-1}, which are predicted to be intense for both SB isomers (see Table 1).

The comparison of the position of the experimental and calculated bands between 1600 and 1750 cm^{-1} further supports the preference for the two SB conformers. Indeed, in these two structures, NH_2 scissoring and the antisymmetric combination of C=O stretches lead to two absorption bands whose calculated positions are in very good agreement with experiment. The broad experimental band presents two maxima at 1656 and 1698 cm^{-1}, very close to the calculated position of the NH_2 scissoring (1637) and C=O stretches (1692−1696), respectively. On the other hand, both CS isomers only have one IR-active mode in this region (the C=O stretch), which should lead to a single maximum in the IRMPD spectrum. Furthermore, the computed position of this mode in CS1 and CS2 is at 1747 cm^{-1}, a frequency at which the experimental signal tends to vanish.

On the basis of this analysis of the relative positions of the experimental and calculated bands, it seems that the two SB conformers, which are computed to be the lowest energy structures for Pro−Na^+, are the best candidates for the interpretation of the experimental spectrum. On the other hand, the difference in relative intensities between the experimental and theoretical spectra (parts a, b, and c in Figure 1, respectively) in the 1600 and 1750 cm^{-1} region might seem large. Considering the proximity of the two normal modes calculated at 1637 and 1696 cm^{-1}, in the case of SB-a, for example, and the strong coupling between the NH_2 scissoring and the antisymmetric CO_2 stretch ($\nu^{as} CO_2$), it is conceivable that the relative contributions of these two local modes to the normal modes are incorrectly described at the present computational level.

It is also conceivable that this apparent discrepancy is due to the multiple photon nature of the IRMPD process. Indeed, as the internal energy increases, the two vibrational transitions are red-shifted to an amount which in this small ion could be of the order of magnitude of the difference between the two frequencies of interest (1637 and 1696 cm^{-1}). As a result, the IRMPD band corresponding to the high-energy mode would be simply red-shifted as compared to the calculated value. On the contrary, a more subtle absorption process could be expected in the case of the low-energy mode. Indeed, as the internal energy increases, the red-shift effect could bring the higher energy mode into resonance with the FEL, thereby enhancing the global multiphoton absorption. As a result, this multiple photon effect will increase the intensity of the lowest energy mode with respect to the highest energy one, as compared to the relative intensities of the linear absorption spectrum calculated assuming that the ion has no internal energy. One could also expect a blue shift of the lowest energy mode and therefore two IRMPD bands closer to each other than the two calculated positions. Such an effect can be observed (see Table 1), but its extent is too small to be meaningfully discussed.

Finally, in light of the above discussion on the relative intensities in the 1600 and 1750 cm^{-1} region, it is interesting to consider the possible contribution of the CS1 isomer to the IRMPD spectrum. As said above, DFT calculations predict that this isomer displays only one band in this region, and it is predicted to be higher in energy than the two vibrational transitions of the SB conformers. As a result, any contribution of CS1 isomer to the IRMPD spectrum would enhance the IRMPD intensity on the blue side of the 1600−1750 cm^{-1} band, which is not observed experimentally.

2. Assignment of the Experimental IR Absorption Spectrum of Gly−Na^+. The IR spectrum of Gly−Na^+ shown in Figure 2a is of somewhat lower quality than that for Pro−Na^+. Still, comparison with the spectra computed for the low-energy isomers of Gly−Na^+ (Figure 2b−d) does provide structural information on the experimentally probed ions. It may be seen that an intense feature exists in the experimental spectrum between 1680 and 1800 cm^{-1} and that all isomers display intense absorption bands in this area, corresponding to C═O stretches. The experimental resolution is too low to permit assignment of this feature to a specific isomer. Absorption between 1150 and 1250 cm^{-1} is also apparent in the experimental spectrum, and the only isomer for which an absorption band exists in this region is CS1 (CS2 only has a weak band, while SB has none). Another clear dichotomy between CS1 on the one hand and CS2 and SB on the other is that absorption intensity in the 1400−1500 cm^{-1} range is weak in the former, in good agreement with experimental results, while it is stronger in the latter two. On the basis of these observations, an assignment of the experimental bands is proposed in Table 2. The most intense observed band may owe its origin to the intense absorption band of νC═O in CS1 at 1759 cm^{-1}, but the $\nu^{as}CO_2$ mode at 1721 cm^{-1} of SB cannot be excluded. The observed band at 1204 cm^{-1} could be assigned to the νC−OH stretch calculated at 1195 cm^{-1} in CS1. Finally, the experimental band with a maximum at 1351 cm^{-1} may be attributed to the superposition of $\tau NH_2 + \tau CH_2$ (calculated at 1359 cm^{-1}) and of $\omega NH_2 + \omega CH_2$ (at 1318 cm^{-1}) of CS1. It is clear overall that the observed bands are only consistent with a dominant population of the CS1 isomer, although a mixture involving SB cannot be ruled out.

V. Conclusions

The coupling of a free electron laser with an FT-ICR mass spectrometer enables recording the infrared spectra of gaseous ions. Although the ion density in the ICR cell is small, the unusually high brightness of the FEL and the temporal structure of its pulses make possible the absorption of multiple IR photons by a large fraction of trapped ions. The broad range of tunability of the FEL offers the possibility of recording IR spectra, thereby obtaining vibrational fingerprints of gaseous ions selectively prepared in an ICR cell. Photon absorption is probed by unimolecular fragmentation processes which are triggered by the accumulation of many vibrational quanta. In this work, we characterized the structural types of Gly−Na^+ and Pro−Na^+ for which all other mass spectrometric methods have failed to date to provide direct and unambiguous structural information. The unimolecular process that reveals absorption is the dissociation of each AA−Na^+ complex into its constituents AA and Na^+. It is remarkable that for both Pro−Na^+ and Gly−Na^+ the IRMPD spectrum is in good agreement with the absorption spectrum predicted by DFT calculations, that is, despite the complicated nature of the IRMPD process, the present approach yields an IR spectrum in close agreement with the absorption features. Furthermore, the method appears to provide access to the lowest energy isomer in each case. The positions of the recorded absorption bands show that the experimental spectrum is consistent with the formation of the salt bridge isomer for Pro−Na^+. In contrast, the experimental spectrum of Gly−Na^+ is consistent with the charge solvation isomer CS1. In this case, however, some population of another isomer cannot be excluded. These results provide the first direct answer to the long-standing question of charge solvation vs salt bridge structure of cationized amino acids. Extending this work to complexes of metal ions with other amino acids and oligopeptides should be relatively straightforward. Therefore, this technique holds great promise for the structural identification of biological molecules by their vibrational fingerprints.

Acknowledgment. We thank Drs. Sophie Bourcier and Martine Caroff for their help in optimizing the MALDI conditions, Luke MacAleese for his help with the MICRA/CLIO setup, and Dr. Jean-Michel Ortega and the CLIO team. We also thank the laser program POLA in Orsay for providing us with an Nd−YAG laser. The reviewers are also acknowledged for their constructive comments.

JA036932V